Metabolic Brain Disease (2018) 33:2039–2044
https://doi.org/10.1007/s11011-018-0312-5

ORIGINAL ARTICLE

Gradual common carotid artery occlusion as a novel model for cerebrovascular Hypoperfusion

Dominic D. Quintana[1] · Xuefang Ren[2,3,4,5] · Heng Hu[1,4] · Elizabeth B. Engler-Chiurazzi[1,2] · Stephanie L. Rellick[1] · Sara E. Lewis[1] · Jessica M. Povroznik[1] · James W. Simpkins[1,4] · Mohammad Alvi[5,6]

Received: 19 January 2018 / Accepted: 12 September 2018 / Published online: 28 September 2018

Abstract

Chronic cerebrovascular hypoperfusion results in vascular dementia and increases predisposition to lacunar infarcts. However, there are no suitable animal models. In this study, we developed a novel model for chronic irreversible cerebral hypoperfusion in mice. Briefly, an ameroid constrictor was placed on the right carotid artery to gradually occlude the vessel, while a microcoil was placed on the left carotid artery to prevent compensation of the blood flow. This procedure resulted in a gradual hypoperfusion developing over a period of 34 days with no cerebral blood flow recovery. Histological analysis of the brain revealed neuronal and axonal degeneration as well as necrotic lesions. The most severely affected regions were located in the hippocampus and the corpus callosum. Overall, our paradigm is a viable model to study brain pathology resulting from gradual cerebrovascular hypoperfusion.

Keywords White matter pathology · Hypoperfusion · Small vessel disease · Gradual vessel occlusion · Cerebral blood flow · Neuronal degeneration

Introduction

Chronic cerebral hypoperfusion is the primary cause of vascular dementia (Kynast et al. 2017), and has been implicated in the development of white matter disease and lacunar infarcts (Black et al. 2009). During the progression of the disease, cerebral arteries harden, resulting in a deficient nutrient delivery to the cerebral parenchyma. This in turn, causes metabolic distress and bioenergetic disturbances that contribute to cerebral degeneration (Vasquez and Zakzanis 2015). There are several models to induce hypoperfusion in experimental animals based on the occlusion of two (Bottiger et al. 1998, 1999), three (Carmichael 2005; Thal et al. 2010; Onken et al. 2012) or four (Pulsinelli and Buchan 1988; Traystman 2003) vessels. However, all these models are based on either permanent or temporal reduction/blockade of blood flow. Therefore, there is a need for a more clinically relevant model that would induce a gradual reduction of cerebral blood flow, and therefore, simulate chronic cerebral hypoperfusion in humans.

In this study, we developed a novel murine model to gradually, and irreversibly reduce cerebral blood perfusion over time. Our paradigm is advantageous because it circumvents the hypoxic/ischemic damage associated with a rapid reduction in CBF observed in other hypoperfusion models (Shibata et al. 2004; Kitamura et al. 2016).

✉ Xuefang Ren
xuren@hsc.wvu.edu

✉ Mohammad Alvi
muhammah.alvi@hsc.wvu.edu

[1] Department of Physiology and Pharmacology, West Virginia University, Morgantown, WV 26506, USA

[2] Department of Neuroscience, West Virginia University, Morgantown, WV 26506, USA

[3] Department of Microbiology, Immunology & Cell Biology, West Virginia University, Morgantown, WV 26506, USA

[4] Experimental Stroke Core, Center for Basic and Translational Stroke Research, West Virginia University, Morgantown, WV 26506, USA

[5] One Medical Center Drive, West Virginia University, Morgantown, WV 26506, USA

[6] Department of Neurology, Center for Basic and Translational Stroke Research, West Virginia University, Morgantown, WV 26506, USA

Materials and methods

Animals

12-14 week-old male C57BL/6 J mice were used. Mice were housed in accordance with Institutional Animal Care and Use Committee (IACUC) guidelines of the West Virginia University (WVU) Health Sciences Center vivarium. Animals were maintained under a light/dark cycle (12:12 h) with food and water available ad libitum. All performed procedures were approved by IACUC of WVU.

Implantation of Ameroid constrictor ring and microcoil

The ameroid constrictor is a device used in veterinary medicine for the treatment of hepatic shunts whereby it induces collateral circulation via blood vessel occlusion. The constrictor ring is composed of a surgical steel ring and an inner layer composed of casein. The hygroscopic property of casein causes its gradual swelling at a predictable rate, wherein the surgical steel ring that surrounds the casein layer forces this swelling inward, resulting in a shrinking inner diameter that gradually occludes blood vessel.

Mice were anesthetized with 4–5% isoflurane and maintained under 1–2% isoflurane in a 30% O_2:70%N_2 mixture and placed on a feedback controlled heating pad to maintain the body temperature at 37 °C. Ophthalmic ointment was placed on the eyes; the surgical area was prepared by trimming the fur and sanitizing the skin with isopropanol pads followed by betadine. Both common carotid arteries (CCAs) were exposed through a midline cervical incision, and an ameroid constrictor ring (cat. MC-0.50-55, Research Instruments SW, CA) was placed around the right CCA following a published protocol (Hattori et al. 2015). A microcoil (cat. SWPA ID 0.18, Wuxi Samini Spring Co., LTD, China) was placed around the left CCA to prevent CBF compensation. The entire surgical procedure was completed within 20 min. The control group received a sham surgery including an incision exposing CCAs but neither the ameroid constrictor rings nor the microcoils were implanted. All further experimentation was performed blinded to surgical group.

Cerebral blood flow measurement

Before the placement of the ameroid constrictor ring and microcoil, baseline CBF was measured. Briefly, the skull was exposed with a 1.5 cm incision. Ten consecutive measurements of CBF were acquired with a MoorFLPI laser Doppler system (Moor Instruments, England) over the course of 5 min with the exposure of 200 ms. To make certain that the surgery did not damage CAA, a second CBF measurement was performed soon after the implantation. The incision was closed with sutures, and the animals were subcutaneously injected with a local anesthetic, bupivacaine (1 mg/kg), once a day for 3 days. Subsequent CBF measurements were performed by reopening the scalp at the same incision site, followed by suturing and bupivacaine injections.

Histochemistry

On day 34, mice were anesthetized and transcardially perfused with 20 mL of 0.01 M phosphate buffered saline followed by 20 mL of 4% paraformaldehyde, pH of 7.45. Brains were extracted, placed in 4% paraformaldehyde and incubated at 4 °C overnight. Fixed brains were sliced into 2 mm coronal sections, embedded in paraffin, sliced into 10 μm coronal sections and mounted onto specimen slides. Deparaffinized and rehydrated tissue sections were stained with Haemotoxylin and Eosin (H&E) to assess general brain pathology (Xiong et al. 2008) and silver stained to assess axonal damage (Uchihara 2007). The sections were imaged on a MIF Olympus VS120 Slide Scanner at 20X magnification.

Statistical analysis

Statistical comparisons were performed using ANOVA (with or without repeated measures, where appropriate). Dunnett's post-hoc test was used for comparison of the experimental groups relative to a control group, or for comparison within a given group at one time point post-surgery (sham or surgical hypoperfusion) relative to the pre-surgery time point. $p < 0.05$ was considered significant.

Results

Cerebral blood flow

Out of the initial seven mice in the hypoperfusion group, two died on day 15 and 17, post-surgery. There was no mortality in the sham group. The impact of surgical hypoperfusion was assessed by measuring changes in global CBF over time (Fig. 1a). To account for group differences in pre-hypoperfusion CBF values, we calculated the percent change at each experimental time point (day 1, 3, 7, 13, 27, and 34) relative to the average of the values at the pre-surgery time point within each group individually (sham or hypoperfusion) (Fig. 1b). One sham animal was excluded from the analyses due to inaccurate CBF measurements at the pre-surgery time point. Using these values, we conducted repeated measures ANOVA with surgery as the independent factor and time point as the repeated factor. There was a significant interaction between these factors [$F(6,63) = 4.967$, $p < 0.0005$]. To determine the extent to which our surgical hypoperfusion model induced a gradual constriction that progressively reduced CBF, we probed

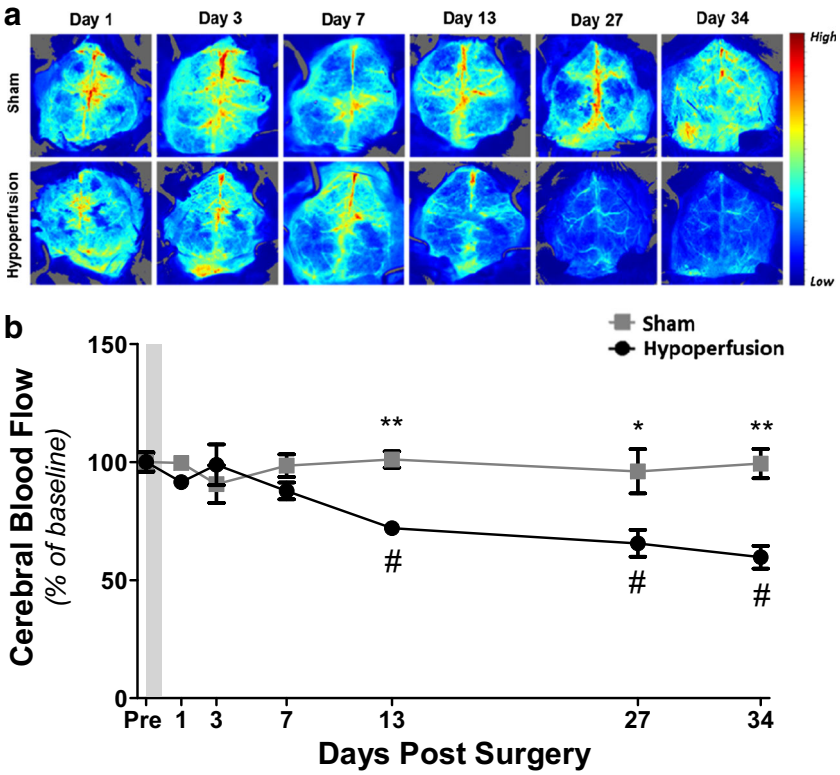

Fig. 1 Cerebral blood flow following induction of surgical hypoperfusion. **a** Laser speckled flowmetry flux images depicting CBF over time. Red color indicates areas of high CBF while blue color indicates areas of low CBF. **b** Temporal changes in CBF measured by the laser Doppler system. Points represent means ± SEM, sham $n = 6$, hypoperfusion $n = 5$, # = $p < 0.05$ for the hypoperfusion group at each time point versus pre-surgical time point; * = $p < 0.05$; ** = $p < 0.001$ between treatment groups at each time point

the significant interaction by evaluating temporal CBF changes within each group separately using the repeated measures ANOVA where time was the repeated factor. For the sham group, the ANOVA was not significant ($p = 0.43$), indicating that there was no change in CBF in this group during the time interval evaluated. However, the repeated measures ANOVA for the surgical hypoperfusion group was significant [$F(6,34) = 10.26$, $p < 0.005$]. To determine critical time points at which

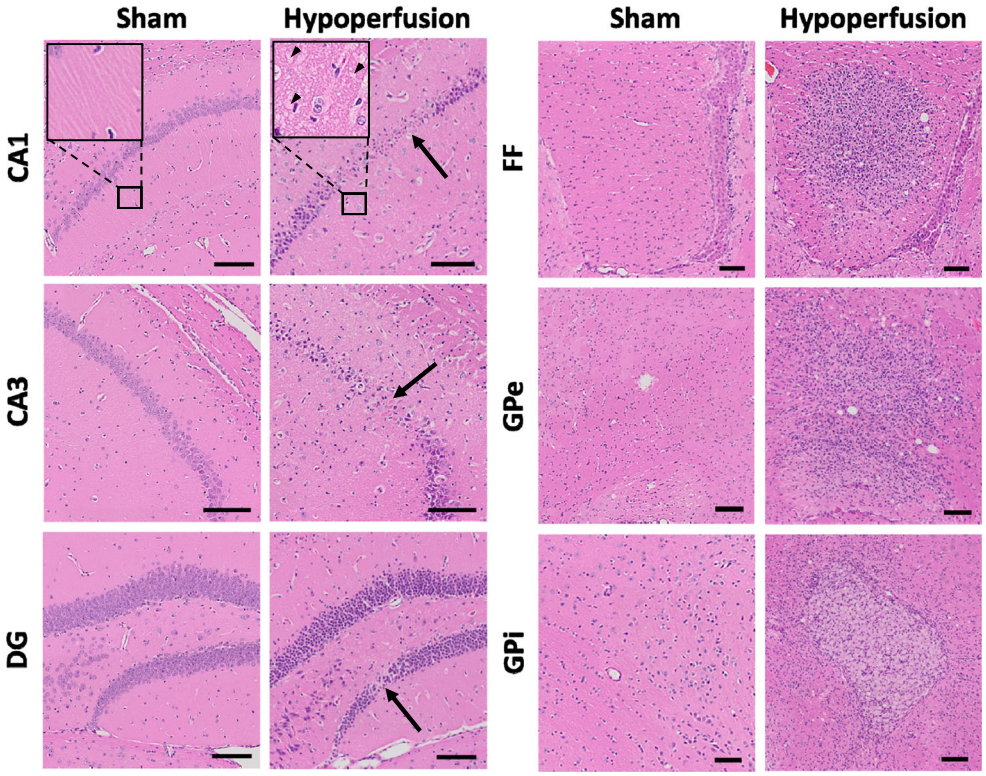

Fig. 2 Cerebrovascular hypoperfusion causes brain tissue injury. Brightfield micrographs of H&E stained coronal tissue sections from sham and hypoperfused group mice. Cornu ammonis 1 (CA1); cornu ammonis 3 (CA3); dentate gyrus (DG); fimbria fornix (FF); globus pallidus externus (GPe); globus pallidus internus (GPi). Arrows indicate regions of neuronal degeneration. In the magnified panel insert, arrowheads indicate vacuolization. Scale bars indicate 100 μm

CBF was altered in this group, and to control for multiple post-hoc two-group comparisons because we were primarily interested in change in CBF relative to the pre-surgery time point, we applied the Dunnett's multiple comparisons approach to assess change in CBF across time. We found no CBF differences at day 1 ($p = 0.07$), day 3 ($p = 0.99$), or day 7 ($p = 0.47$) from the pre-surgery time point in the hypoperfusion group. However, CBF in the hypoperfusion group was significantly decreased from the pre-surgery time point by 28% on day 13 ($p = 0.04$), 43% on day 27 ($p = 0.04$) and 40% on day 34 ($p = 0.02$). The gradual reduction in CBF was further supported by a significant drop in CBF in the hypoperfusion mice as compared to sham mice at day 13 ($p = 0.0001$), day 27 ($p = 0.02$), and day 34 ($p = 0.0008$). There were no differences in CBF between these groups on days 1, 3 and 7 post-surgery.

Histological assessment of cerebral injury

H&E staining of cerebral tissue from hypoperfused animals revealed a variety of hallmark pathologies of gray and white matter (Fig. 2). Thus, there was striking neuronal loss in the stratum pyramidale of the Cornu Ammonis 1 (CA1) and Cornu Ammonis 3 (CA3) region of the hippocampus, and loss of neurons in the stratum granulosum in the dentate gyrus (DG). We noticed hemisphere asymmetry in hippocampal and cortical injury in hypoperfused mice. Hypoperfusion is known to induce lesions that are formed by localized intense vacuolization (Wells and Wells 1989). We observed lesions of intense vacuolization in the stratum oriens, stratum pyramidale, and stratum radiatum in the CA1 and CA3 regions of the hippocampus. There were overt degenerative lesions in the fimbria of the fornix (FF), external segment of the globus pallidus (GPe), and internal segment of the globus pallidus (GPi). These lesions contained an elevated number of nuclei, suggesting infiltration of inflammatory cells. No pathology was evident in the sham group.

Silver staining revealed severe axonal injury, identified as punctate staining observed in the stratum oriens and stratum radiatum of the CA1 region of the hippocampus of hypoperfused mice (Fig. 3). A similar observation was made in the CA2 region. Axonal injury in both the stratum oriens and stratum radiatum of the CA3 region of the hippocampus appeared to be less affected.

Silver staining also revealed prominent injury of the corpus callosum in hypoperfused mice (Fig. 4). Severe atrophy of the body of the corpus callosum was apparent in the hypoperfused mice. Intense silver staining of axons projecting through the corpus callosum indicated axonal damage. The appearance of gaps between axons in the corpus callosum indicated their degeneration. Additionally, axonal disorganization was a common observation in regions with extensive axonal injury. No axonal injury was apparent either in the hippocampus or in the corpus callosum of the sham mice.

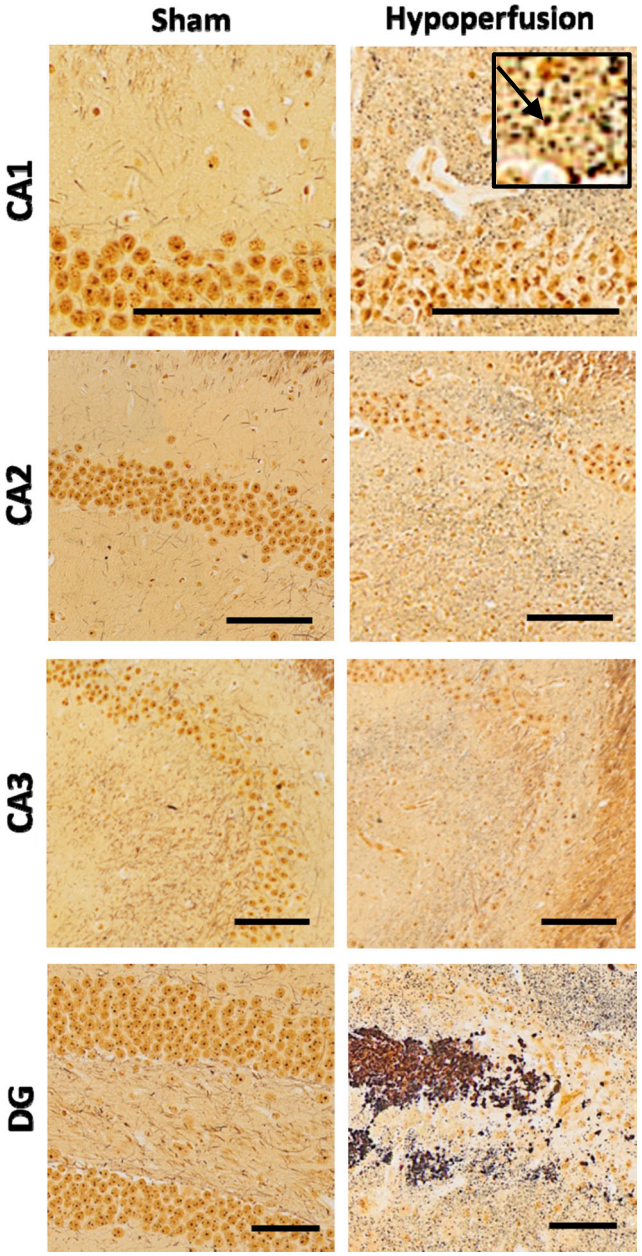

Fig. 3 Cerebrovascular hypoperfusion causes hippocampal injury. Sliver stained tissue depicting histological changes in sham and hypoperfusion group mice. Cornu ammonis 1 (CA1); cornu ammonis 2 (CA2); cornu ammonis 3 (CA3); dentate gyrus (DG). The magnified panel insert shows degenerated axons and their punctated appearance (black arrow). Scale bars indicate 100 μm

Discussion

Numerous studies of cerebral pathophysiology of hypoperfusion in animal models have led to the identification of hundreds of potential therapeutic compounds. However, in clinical trials, all of these compounds have proven ineffective, or less effective than the already clinically available interventions. The lack of adequate experimental models of cerebrovascular hypoperfusion with pathophysiology analogous to

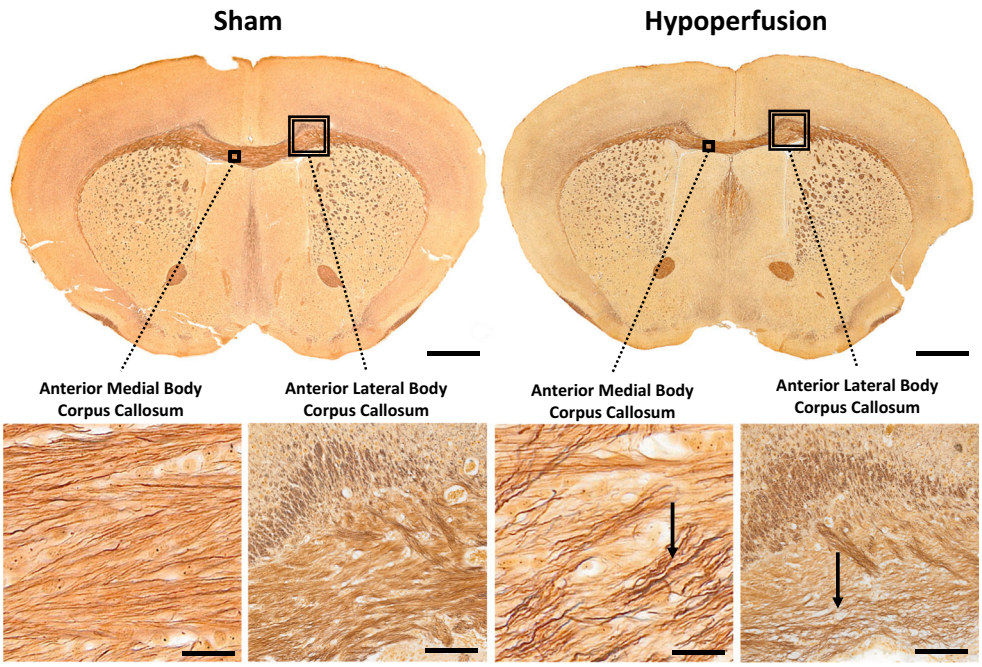

Fig. 4 Cerebrovascular hypoperfusion causes corpus callosum injury. Silver stained whole coronal tissue sections of the brain and magnified regions of the medial and lateral corpus callosum in sham and hypoperfused mice. Black arrows in the medial and lateral corpus callosum indicate axonal degeneration (threadlike) and disorganization (intense and non-bundled), respectively. Scale bars indicate 1 mm in the whole coronal sections, and 20 μm in the magnified panels

humans is likely the primary cause of the loss of translation from laboratory to clinical practice. A major limitation of the current animal models is variable severity of ischemic damage that weakens the statistical power of experimental research making the identification of effective therapeutics difficult.

There are several paradigms to induce cerebrovascular hypoperfusion in mice. Essentially all of the current paradigms involve the occlusion of two (Bottiger et al. 1998, 1999), three (Carmichael 2005; Thal et al. 2010; Onken et al. 2012) or four (Pulsinelli and Buchan 1988; Traystman 2003) vessels. These paradigms include, bilateral common carotid artery stenosis (Shibata et al. 2007; Matin et al. 2016; Patel et al. 2017), permanent carotid artery ligation (Ohta et al. 1997) and sequential common carotid artery occlusion (Cechetti et al. 2010). Limitations of other procedures used to induce hypoperfusion in mice include a high mortality rate (Longa et al. 1989; Connolly Jr et al. 1996; Kitagawa et al. 1998) and inconsistency in the severity and localization of cerebral damage (Connolly Jr et al. 1996; Clark et al. 1997; Ohta et al. 1997; Takano et al. 1997; Matin et al. 2016; Patel et al. 2017). Using the present paradigm, we were able to induce a consistent time-dependent reduction of cerebral blood flow that resulted in limited mortality and relatively conserved damage severity and localization.

Models of cerebrovascular hypoperfusion that use bilateral CCA stenosis with microcoils have demonstrated pathology to white matter without gray matter damage after 30 days of chronic reduction of CBF (Shibata et al. 2004). However, a maximum reduction of CBF to approximately 50% of baseline occurred within 2 h post-surgery, followed by a progressive recovery of CBF to approximately 80% of baseline by day 30 (Shibata et al. 2004). Also, a similar acute reduction of CBF to ~50% of baseline was observed on the first day in other studies (Kitamura et al. 2016; Srinivasan et al. 2015; Hattori et al. 2016). Growth of collateral vessels occurs only after a few days of hypoperfusion resulting in a recovery of CBF over time (Srinivasan et al. 2015). This suggests that the greatest damage occurs during the first days after surgery, and once CBF is restored, the tissue recovers. This makes it difficult to gauge accurately the extent of damage caused by permanently reduced blood flow as in cerebral hypoperfusion in humans. In our model, the stenosis of the CCA develops gradually over time. The irreversibility of CBF reduction prevents the recovery of cerebral tissue, which may explain the injury of both the white and gray matter.

In hypertensive rats a two-vessel occlusion with ameroid constrictor rings of both CCAs CBF was reduced by approximately 20% within 3 h, and reached a maximum of 70% after 24 h (Kitamura et al. 2016). This CBF reduction persisted for seven days, but recovered to approximately 80% of baseline by day 14. In contrast, we found no change in CBF for seven days post-surgery in the hypoperfusion group. Moreover, CBF was gradually reduced beginning day 13, and reached 60% of baseline on day 34. There was no CBF recovery over the 34 days of hypoperfusion. In agreement with the findings of Kitamura et al. (2016) we found similar lesion in the corpus callosum. However, we also observed severe damage to the hippocampus, cortex and subcortical regions. Albeit asymmetric to the brain. These pathological differences may be attributed to the characteristic hemodynamic properties of hypertensive rats used by Kitamura et al.

In conclusion, we have established a novel murine model of irreversible hypoperfusion that develops gradually. Our paradigm results in a substantial reduction of CBF and

produces consistent localization and severity of cerebral injury in the hippocampus, cortex, fornix, globus pallidus and corpus callosum with a relatively low mortality rate. The model provides a tool for investigating cerebral vascular disease with chronic cerebral hypoperfusion, which is implicated in the development of white matter disease and lacunar infarcts.

Acknowledgements The authors thank Dr. Gregory Konat for revising and editing the manuscript. This study was supported by the Helen Marie Lewis Medical Research Foundation (to JWS, XR, and AM), NIH CoBRE (P20 GM109098 to JWS), AHA SDG (16SDG31170008 to XR), NIH T32 (AG052375 to JWS), and funding from the Department of Neurology at WVU (to AM).

References

Black S, Gao F, Bilbao J (2009) Understanding white matter disease: imaging-pathological correlations in vascular cognitive impairment. Stroke 40:S48–S52

Bottiger BW, Schmitz B, Wiessner C, Vogel P, Hossmann KA (1998) Neuronal stress response and neuronal cell damage after cardiocirculatory arrest in rats. Brain Res Mol Brain Res 18:1077–1087

Bottiger BW, Teschendorf P, Krumnikl JJ, Vogel P, Galmbacher R, Schmitz B, Motsch J, Martin E, Gass P (1999) Global cerebral ischemia due to cardiocirculatory arrest in mice causes neuronal degeneration and early induction of transcription factor genes in the hippocampus. Brain Res Mol Brain Res 65:135–142

Carmichael ST (2005) Rodent models of focal stroke: size, mechanism, and purpose. NeuroRx 2:396–409

Cechetti F, Worm PV, Pereira LO, Siqueira IR, AN C (2010) The modified 2VO ischemia protocol causes cognitive impairment similar to that induced by the standard method, but with a better survival rate. Braz J Med Biol Res 43:1178–1183

Clark WM, Lessov NS, Dixon MP, Eckenstein F (1997) Monofilament intraluminal middle cerebral artery occlusion in the mouse. Neurol Res 19:641–648

Connolly ES Jr, Winfree CJ, Stern DM, Solomon RA, Pinsky DJ (1996) Procedural and strain-related variables significantly affect outcome in a murine model of focal cerebral ischemia. Neurosurgery 38:523–531 discussion 532

Hattori Y, Enmi J, Kitamura A, Yamamoto Y, Saito S, Takahashi Y, Iguchi S, Tsuji M, Yamahara K, Nagatsuka K, Iida H, Ihara M (2015) A novel mouse model of subcortical infarcts with dementia. J Neurosci 35:3915–3928

Hattori Y, Enmi J, Iguchi S, Saito S, Yamamoto Y, Nagatsuka K, Iida H, Ihara M (2016) Substantial reduction of parenchymal cerebral blood flow in mice with bilateral common carotid artery stenosis. Sci Rep 6:32179

Kitagawa K, Matsumoto M, Yang G, Mabuchi T, Yagita Y, Hori M, Yanagihara T (1998) Cerebral ischemia after bilateral carotid artery occlusion and intraluminal suture occlusion in mice: evaluation of the patency of the posterior communicating artery. J Cereb Blood Flow Metab 18:570–579

Kitamura A, Saito S, Maki T, Oishi N, Ayaki T, Hattori Y, Yamamoto Y, Urushitani M, Kalaria RN, Fukuyama H, Horsburgh K, Takahashi R, Ihara M (2016) Gradual cerebral hypoperfusion in spontaneously hypertensive rats induces slowly evolving white matter abnormalities and impairs working memory. J Cereb Blood Flow Metab 36:1592–1602

Kynast J, Lampe L, Luck T, Frisch S, Arelin K, Hoffmann KT, Loeffler M, Riedel-Heller SG, Villringer A, Schroeter ML (2017) White matter hyperintensities associated with small vessel disease impair social cognition beside attention and memory. Journal of cerebral blood flow and metabolism : official journal of the International Society of Cerebral Blood Flow and Metabolism:271678X17719380

Longa EZ, Weinstein PR, Carlson S, Cummins R (1989) Reversible middle cerebral artery occlusion without craniectomy in rats. Stroke 20:84–91

Matin N, Fisher C, Jackson WF, Dorrance AM (2016) Bilateral common carotid artery stenosis in normotensive rats impairs endothelium-dependent dilation of parenchymal arterioles. Am J Phys Heart Circ Phys 310:H1321–H1329

Ohta H, Nishikawa H, Kimura H, Anayama H, Miyamoto M (1997) Chronic cerebral hypoperfusion by permanent internal carotid ligation produces learning impairment without brain damage in rats. Neuroscience 79:1039–1050

Onken M, Berger S, Kristian T (2012) Simple model of forebrain ischemia in mouse. J Neurosci Methods 204:254–261

Patel A, Moalem A, Cheng H, Babadjouni RM, Patel K, Hodis DM, Chandegara D, Cen S, He S, Liu Q, Mack WJ (2017) Chronic cerebral hypoperfusion induced by bilateral carotid artery stenosis causes selective recognition impairment in adult mice. Neurol Res 39:910–917

Pulsinelli WA, Buchan AM (1988) The four-vessel occlusion rat model: method for complete occlusion of vertebral arteries and control of collateral circulation. Stroke 19:913–914

Shibata M, Ohtani R, Ihara M, Tomimoto H (2004) White matter lesions and glial activation in a novel mouse model of chronic cerebral hypoperfusion. Stroke 35:2598–2603

Shibata M, Yamasaki N, Miyakawa T, Kalaria RN, Fujita Y, Ohtani R, Ihara M, Takahashi R, Tomimoto H (2007) Selective impairment of working memory in a mouse model of chronic cerebral hypoperfusion. Stroke 38:2826–2832

Srinivasan VJ, Yu E, Radhakrishnan H, Can A, Climov M, Leahy C, Ayata C, Eikermann-Haerter K (2015) Micro-heterogeneity of flow in a mouse model of chronic cerebral hypoperfusion revealed by longitudinal Doppler optical coherence tomography and angiography. J Cereb Blood Flow Metab 35:1552–1560

Takano K, Tatlisumak T, Bergmann AG, Gibson DG 3rd, Fisher M (1997) Reproducibility and reliability of middle cerebral artery occlusion using a silicone-coated suture (Koizumi) in rats. J Neurol Sci 153:8–11

Thal SC, Thal SE, Plesnila N (2010) Characterization of a 3-vessel occlusion model for the induction of complete global cerebral ischemia in mice. J Neurosci Methods 192:219–227

Traystman RJ (2003) Animal models of focal and global cerebral ischemia. ILAR J 44:85–95

Uchihara T (2007) Silver diagnosis in neuropathology: principles, practice and revised interpretation. Acta Neuropathol 113:483–499

Vasquez BP, Zakzanis KK (2015) The neuropsychological profile of vascular cognitive impairment not demented: a meta-analysis. J Neuropsychol 9:109–136

Wells GA, Wells M (1989) Neuropil vacuolation in brain: a reproducible histological processing artefact. J Comp Pathol 101:355–362

Xiong Y, Mahmood A, Lu D, Qu C, Kazmi H, Goussev A, Zhang ZG, Noguchi CT, Schallert T, Chopp M (2008) Histological and functional outcomes after traumatic brain injury in mice null for the erythropoietin receptor in the central nervous system. Brain Res 1230:247–257